NASA Contractor Report 181955
ICASE Report No. 89–51

ICASE

OPTIMUM SHAPE OF A BLUNT FOREBODY IN HYPERSONIC FLOW

L. Maestrello
L. Ting

Contract No. NAS1–18605
December 1989

Institute for Computer Applications in Science and Engineering
NASA Langley Research Center
Hampton, Virginia 23665–5225

Operated by the Universities Space Research Association

National Aeronautics and Space Administration
Langley Research Center
Hampton, Virginia 23665-5225

OPTIMUM SHAPE OF A BLUNT FOREBODY IN HYPERSONIC FLOW

L. Maestrello
NASA Langley Research Center
Hampton, VA 23665

L. Ting[1]
Courant Institute of Mathematical Sciences
New York University
New York, NY 10012

ABSTRACT

The optimum shape of a blunt forebody attached to a symmetric wedge or cone is determined. The length of the forebody, its semi-thickness or base radius, the nose radius and the radius of the fillet joining the forebody to the wedge or cone are specified. The optimum shape is composed of simple curves. Thus experimental models can be built readily to investigate the utilization of aerodynamic heating for boundary layer control. The optimum shape based on the modified Newtonian theory can also serve as the preliminary shape for the numerical solution of the optimum shape using the governing equations for a compressible inviscid or viscous flow.

[1]Research was supported by the National Aeronautics and Space Administration under NASA Contract No. NAS1-18605 while the second author was in residence at the Institute for Computer Applications in Science and Engineering (ICASE), NASA Langley Research Center, Hampton, VA 23665.

1. INTRODUCTION

Optimum shapes of two dimensional or axi-symmetric bodies in hypersonic flight were studied in the early stage of hypersonic flow research. The results were summarized in the book [1] by Hayes and Probstein. The analyses were based on the Newtonian-Busemann (N-B) theory which was justified as the leading term of an asymptotic solution at large upstream Mach number. Shapes of minimum wave drag with given body length, thickness and/or volume were determined. The minimum wave drag is achieved when the product $P_1 \cos\theta_1$ is a maximum where θ_1 is the inclination of the surface at the rear end with respect to the free stream while P_1 is an integral along the surface from the front to the rear and depends on the shape. With the assumption that θ_1 and P_1 are independent of each other, the "absolute" optimum shape which maximize the integral P_1 has to fulfill also the end condition

$$\theta_1 = 0. \tag{1}$$

This end condition cannot be met without a discontinuity in slope. Engineering designs using an absolute optimum forebody followed by a body confined within a free surface were proposed to achieve a "proper" shaped body with a wave drag somewhat higher than that of the optimum shape. We also note that the optimum forebody has a sharp leading edge or a conical nose [1].

It is well known that the rate of heat transfer to a "cold" wall at the stagnation point is inversely proportional to the square root of the nose radius [2-4]. An optimum shape with a sharp or pointed forebody is not suitable for hypersonic flight. To reduce the aerodynamic heating to an allowable limit, a body in hypersonic flight has to have a finite radius of curvature, R_0, at the stagnation point. The minimum radius depends of course on the flight Mach number M_∞, the altitude and the physical properties of the nose with or without a heat shielding device. An optimum forebody has to have a nose with a prescribed radius of curvature greater than the minimum.

In recent studies on boundary layer control by surface heating or cooling [5-8]. It was found that a boundary layer which is heated upstream and/or cooled downstream is more stable than that without thermal control. In a hypersonic flow, the aerodynamic heating near the stagnation point provides a nature source for heating the boundary layer. The amount of heat acquired by the boundary layer is proportional to $R_0^{j+\frac{3}{2}}$, where $j = 0$ and 1 for two dimensional and axi-symmetric flow respectively. From the point of view of boundary layer control, it is also desirable to have a nose with a prescribed radius of curvature R_0 and then find the optimum shape.

It is well known that the modified Newtonian theory [1], although an empirical theory,

has been employed in engineering designs because its prediction of surface pressure is in much better agreement with the experimental data than the N-B theory. We shall use the modified Newtonian theory to compute the wave drag and find the optimum shape in this report. To avoid flow separation or shock boundary layer interaction, we require that the optimum contour should be smooth, that is, it should match with the circular nose in the front and the wedge or cone in the rear without a discontinuity in slope. As we shall see in the next section, the optimum shape under the modify Newtonian theory does not call for the rear end condition (1). However, the slope of the optimum forebody in general will not match with that of the wedge or cone. To remove the discontinuity in slope we assume that the forebody is joined smoothly to the wedge or cone via a fillet of radius R_1. Thus we complete the specifications of the free front and rear end conditions for the optimum contour.

2. THE OPTIMUM SHAPE

The modified Newtonian theory is the direct application of the Newtonian theory along the surface with a correction factor such that the correct stagnation pressure p_s is obtained. The surface pressure p is related to the inclination of the surface with the upstream flow, θ, by

$$p = p_s \sin^2 \theta. \tag{2}$$

The wave drag of the forebody is

$$D = 2p_s \int_0^h \sin^2 \theta \, (\pi y)^j dy, \tag{3}$$

where h is the semi-thickness or base radius. With $dx = dy \cot \theta$, the length of the forebody l yields a constraint,

$$l = \int_0^h \cot \theta \, dy. \tag{4}$$

Figure 1 shows the front and the rear end of the forebody located at $x = -l$ and $x = 0$ respectively. The centers for the circular nose and the fillet are located at $C_0(-l + R_0, 0)$ and $C_1(-R \sin \beta, h + R \cos \beta)$, where β denotes the half wedge angle or cone angle. Here we have assumed that the nose is convex with $R_0 > 0$ while the fillet can be concave for $R_1 > 0$ or convex for $R_1 > 0$.

The parametric equations for the circular nose and fillet are

$$x = (-l + R_0) - R_0 \sin \theta_n, \tag{5}$$

$$y = R_0 \cos \theta_n, \tag{6}$$

for $0 \leq y \leq y_0$ and

$$x = -R_1 \sin\beta + R_1 \sin\theta_f \tag{7}$$

$$y = (h + R_1 \cos\beta) - R_1 \cos\theta_f \tag{8}$$

for $h \geq y \geq y_1$. The shape function $\theta_n(y)$ along the circular nose and $\theta_f(y)$ along the fillet are defined by (6) and (8). The shape function of the contour, $\theta(y)$ for $y_0 \geq y \geq y_1$, and its two free ends, y_0 and y_1, shall be defined by the necessary conditions for minimum wave drag subject to the constraint (4). We introduce the Lagrange multiplier λ and then seek to minimize

$$\Phi(\epsilon_1, \epsilon_2, \epsilon) = \frac{D}{2p_s\pi^j} - \lambda l = \int_0^{\bar{y}_0} dy\,(\sin^2\theta_n - \lambda\cot\theta_n) + \int_{\bar{y}_0}^{\bar{y}_1} dy\,(\sin^2\bar{\theta} - \lambda\cot\bar{\theta}) + \int_{\bar{y}_1}^{h} dy\,(\sin^2\theta_f - \lambda\cot\theta_f), \tag{9}$$

where ϵ_1, ϵ_2 and $\epsilon\eta(y)$ denote the variations of y_0, y_1, and $\theta(y)$, i.e.,

$$\bar{y}_0 = y_0 + \epsilon_0, \quad \bar{y}_1 = y_1 + \epsilon_1 \quad \text{and}$$

$$\bar{y} = \theta(y) + \epsilon\eta(y) \quad \text{for} \quad \bar{y}_0 \leq \bar{y} \leq \bar{y}_1. \tag{10}$$

The necessary conditions for a minimum Φ are

$$\theta(y_0^+) = \theta_n(y_0^-), \tag{11}$$

$$\theta(y_1^-) = \theta_f(y_1^+) \tag{12}$$

and

$$y^j \sin^3\theta = \text{constant } hC. \tag{13}$$

Condition (4) is fulfilled on account of (5) and (6). Equations (11) and (12) are the natural end conditions, requiring that the optimum contour joins smoothly with the circular nose at y_0 and the fillet at y_1. Equation (13) says that θ remains constant for $y_0 \leq y \leq y_1$ for two dimensional cases and $\sin\theta \sim y^{-1/3}$ for axi-symmetric cases.

The optimum forebody, defined by (5-8), (11), (12) and (13), depends on four parameters $\bar{R}_0, \bar{R}_1, \bar{l}$ and β with

$$\bar{R}_0 = R_0/h, \quad \bar{R}_1 = \bar{R}_1/h \text{ and } \bar{l} = l/h. \tag{14}$$

In order to study the ranges of these four parameters and their effects on the wave drag, we introduce a reference forebody as shown in Fig. 2. It is composed of the extension of the wedge (or conical) surface matched with the circular (or spherical) nose of radius R_0. Hence, we have the shape function

$$\theta^*(y) = \beta \text{ for } h \geq y \geq y_1 = y_0^* = R_0\cos\beta \tag{15}$$

and

$$\theta^*(y) = \cos^{-1}(y/R_0) \text{ for } y_0^* \geq y \geq 0. \tag{16}$$

The scaled length of the forebody is

$$\bar{l}^* = \cos\beta + \bar{R}_0\,(1 - \cos\beta). \tag{17}$$

This configuration implies that $\bar{R}_0 \cos\beta < 1$. This is fulfilled in real problems for which $\bar{R}_0 < 1$. Its scaled wave drag is

$$\frac{D^*}{2p_s h(\pi h)^j} = \frac{\sin^2\beta}{1+j}[1 - (\bar{R}_0\cos\beta)^{1+j}] + (\bar{R}_0\cos\beta)^{1+j}[\frac{1}{1+j} - \frac{\cos^2\beta}{3+j}]. \tag{18}$$

Also shown in Fig. 2 is an optimum two dimensional forebody with the same $\bar{\beta}$, $\bar{R}_0$ and h and a convex fillet, ($\bar{R}_1 < 0$). The optimum shape is convex with

$$\theta(0) = \pi/2, \quad \theta(h) = \beta \quad \text{and} \quad \theta'(y) < 0, \tag{19}$$

for $0 \le y \le h$. In particular, we note that at the point of tangency with the circular nose,

$$\theta(y_0) > \beta \qquad \text{hence} \qquad y_0 < y^* \tag{20}$$

and that

$$\theta(y) > \cos^{-1}(y/R_0), \tag{21}$$

for $y_0 < y < y^*$. It follows from (19), (20) and (21) that

$$\theta(y) > \theta^*(y) \quad \text{for} \quad 0 < y < h, \tag{22}$$

and from (3) and (4) that,

$$D > D^* \quad \text{and} \quad l < l^*. \tag{23}$$

Thus we conclude:

> *I, The wave drag of an optimum forebody with a convex fillet, $R_1 < 0$, is greater than the wave drag D^* of the corresponding reference forebody, i.e., having the same β, R_0 and h, while the length of the former is shorter than the length l^* of the latter.*

The reference forebody can be considered as the limiting optimum forebody as $\bar{R}_1 \to -\infty$ while $y_1 \to y_0$.

From hereon, we consider only the optimum forebody with a concave fillet, i.e.,

$$R_1 > 0 \tag{24}$$

and study the drag reduction relative to the drag D^* of the corresponding reference forebody as $\bar{R}_1$ decreases and $\bar{l}$ increases. We shall treat the two dimensional and the axi-symmetric problems separately in the following two sections. In each section we determine the following:

1. The optimum contour and the points of the tangency of the contour with the circular nose and the convex fillet for a given set of $\bar{R}_0, \bar{R}_1, \bar{l}$ and β.

2. The upper and lower bounds of the scaled length $\bar{l}$ as functions of $\bar{R}_0, \bar{R}_1$ and β.

3. The dependence of the wave drag on those parameters.

3. TWO DIMENSIONAL OPTIMUM FOREBODIES

For $j = 0$, Eq. (13) for the optimum contour yields

$$\theta = \text{constant } \alpha \quad \text{for} \quad y_0 \leq y \leq y_1. \tag{25}$$

The optimum forebody is composed of the circular nose, for $0 \leq y \leq y_0$, and the concave circular fillet, for $y_1 \leq y \leq h$, joined together by their common tangent T_0T_1, where T_0 and T_1 denote the points of tangency at $y = y_0$ and $y = y_1$, respectively, (see Fig. 2). Instead of solving for α, y_0 and y_1 from Eqs. (5-8), (11), (12) and (25), we determine them directly by making use of elementary geometry. Let C_0C_2 be the straight line parallel to T_0T_1 intersecting the radial line C_1T_1 at C_2. Then points C_0C_2 and C_1 are the vertices of a right triangle with

$$|C_1C_2| = R_0 + R_1. \tag{26}$$

Let ψ and τ denote $\angle C_2C_0C_1$ and $\angle OC_0C_1$ respectively. We obtain from Fig. 2 the following:

$$\begin{aligned} &\psi = \sin^{-1}[(R_1 + R_0)]/|C_0C_1|, \\ &\tau = \sin^{-1}[(h + R_1\cos\beta)]/|C_0C_1|, \\ &\beta > \alpha = \tau - \psi > 0, \\ \text{with} \quad &|C_0C_1|^2/h^2 = (\bar{l} - \bar{R}_0 - \bar{R}_1\sin\beta)^2 + (1 + \bar{R}_1\cos\beta)^2. \end{aligned} \tag{27}$$

Note that the angles ψ, τ and α are functions of $\bar{l}, \bar{R}_0, \bar{R}_1$ and β and $\psi < 0$ in Fig. 2 since $-R_1 > R_0 > 0$. The solutions are real so long as $|C_0C_1| \geq R_1 + R_0$.

When $\bar{l}$ is equal to $\bar{l}^*$ of the reference forebody, Eq. (17), we have $\alpha = \beta$ and $y_1 = h$ for all $R_1 > 0$, keeping in mind that $\bar{R}_0\cos\beta < 1$. For an optimum contour we have $\alpha < \beta$, $y_1 < h$ and hence $\bar{l} > \bar{l}^*$.

If the ordinate of the center C_1 of the fillet is greater than or equal to $R_1 + R_2$, i.e.,

$$1 + \bar{R}_1\cos\beta \geq \bar{R}_1 + \bar{R}_0, \tag{28}$$

it is evident from (27) that $|C_0C_1| > R_1 + R_2$ and $\alpha > 0$ and that as $\bar{l}$ increases from $\bar{l}^*$ to ∞, α decreases from β to 0.

On the other hand if (28) is not true, we have an upper bound for $\bar{l}$ defined by the condition $|C_1C_0| = R_1 + R_0$. The upper bound is

$$\bar{l}_m = \bar{R}_1 \sin\beta + \bar{R}_0 - \{(\bar{R}_1 + \bar{R}_0)^2 - (1 + \bar{R}_1 \cos\beta)\}^{1/2}. \tag{29}$$

When the length reaches its maximum, we have $\theta_0 = \theta_1 = \theta_m = \cos^{-1}[(1 + \bar{R}_1 \cos\beta)/(\bar{R}_1 + \bar{R}_0)]$.

As the length l increases from $\bar{l}^*$ to $\bar{l}_m$, θ_1 decreases from β to θ_m. We thereby conclude that,

II, An optimum shape defined by the equations in (27) exists for a scaled length $\bar{l} \geq \bar{l}^*$, when condition (28) holds and for $\bar{l}_m \geq \bar{l} \geq \bar{l}*$ when (28) does not.

With α defined by (27), the coordinates of the points of tangency are defined by (17) and (18). The results are $T_0(-l + R_0 - R_1 \sin\alpha, R_0 \cos\alpha)$ and $T_1(-R_1 \sin\beta + R_1 \sin\alpha, h + R_1 \cos\beta - R_1 \cos\alpha)$. The scaled wave drag of the optimum forebody is

$$\bar{D}(\bar{l}, \bar{R}_0, \bar{R}_1, \beta) = \frac{D}{2p_s h} = \bar{D}_0 + \bar{D}_f + \bar{D}_n, \tag{30}$$

where

$$\bar{D}_0 = \bar{R}_1[\cos\alpha(1 - \frac{\cos^2\alpha}{3}) - \cos\beta(1 - \frac{\cos^2\beta}{3}],$$

$$\bar{D}_f = \sin^2\alpha[1 + \bar{R}_1 \cos\beta - (\bar{R}_0 + \bar{R}_1)\cos\alpha]$$

and

$$\bar{D}_n = \bar{R}_0 \cos\alpha[1 - \frac{\cos^2\alpha}{3}].$$

Here $\bar{D}_0, \bar{D}_f$ and $\bar{D}_n$ denote the scaled wave drags of the optimum contour, the fillet and the nose. For hypersonic configurations, we have $\beta << 1$. With $\alpha \leq \beta$, we have $\bar{D}_0 = 0(\beta^2)$, $\bar{D}_f = 0(\beta^2)$ and $\bar{D}_n = \frac{2}{3}\bar{R}_0 + 0(\bar{R}_0\beta^2)$. If the nose radius is not very small, $\bar{R}_0 \gg \beta^2$, the wave drag of an optimum forebody is dominated by that of its nose, D_n. and is only slightly less than that of the reference forebody by $O(\beta^2)$. Since the scaled wave drag of a wedge of semi angle β ($\bar{R}_0 = 0$) is $\sin^2\beta$, the scaled wave drag of an optimum forebody will be greater than that of the wedge unless $\bar{R}_0$ is very small, $0(\beta^2)$. For example, for a 4° half angle, $\beta^2 = 0.005$ we have $R_0/h \sim 0.005$ which will be too small and most likely be ruled out due to aerodynamic heating.

Consider two optimum forebodies having the same β, R_0, R_1 and h but different lengths l and $\tilde{l}$, as shown in Fig. 2. It is evident that the one which has the shorter length $\tilde{l}$ has larger wave drag since $\tilde{\theta}(y) \geq \theta(y)$. As the length l decreases the inclination of the common tangent α increases. When α reaches the upper bound β, y_1 is equal to h and the optimum forebody coincides with the reference forebody of length $l*$ with wave drag $D*$, which is independent of the fillet radius R_1. Again we note that the differences will be only $O(\beta^2)$ unless the scaled nose radius is very small. Thus we conclude:

III, The wave drag of an optimum forebody with $R_1 > 0$ is less than the wave drag D^* of the reference forebody having the same β, R_0 and h while the length of the former is longer than the length l^* of the latter.

IV, If the nose radius is not very small, $\bar{R}_0 \gg \beta^2$, the wave drag of an optimum forebody is dominated by that of its nose, D_n and the reduction in the scaled wave drag for a longer forebody, $l > l^*$, will be only $O(\beta^2)$.

4. AXI-SYMMETRIC OPTIMUM FOREBODIES

In this section we seek the answers to the three items listed at the end of **Sec. 3** for the axi-symmetric problems. In contrast to the two dimensional problems, we find that for each set of $\bar{R}, \bar{R}_1, \bar{R}_0, \beta$ and $\bar{l}$, with $\bar{l}$ lying within its upper and lower bounds, there are two optimum forebodies, called type *a* and *b*. The characteristics of these two types are studied in detail. For $j = 1$, Eq. (13) for the optimum contour becomes

$$y \sin^3\theta = hC \quad \text{for} \quad y_0 \le y \le y_1, \tag{31}$$

where
$$hC = y_0 \sin^3\theta_0 = y_1 \sin^3\theta_1. \tag{32}$$

From (6), (8) and (32) we obtain an equation for θ_0 and θ_1. It is

$$\bar{R}_0 \cos\theta_0 \sin^3\theta_0 = C = (1 + \bar{R}_1 \cos\beta - \bar{R}_1 \cos\theta_1) \sin^3\theta_1. \tag{33}$$

From (4), (5) and (6) we get the second equation,

$$\begin{aligned} &\bar{l} + \bar{R}_0(1 - \sin\theta_0) - \bar{R}_1(\sin\beta - \sin\theta_1) \\ &\quad = [1/h] \int_{y_0}^{y_1} \cot\theta \, dy = [3/8]C[g(\theta_1) - g(\theta_0)], \end{aligned} \tag{34}$$

where
$$g(\theta) = 2\csc^3\theta \, \cot\theta - \csc\theta \, \cot\theta - \log\cot[\theta/2].$$

Since the optimum shape defined by (31) is convex while the fillet is concave, they can come in contact at only one point, if they do. That is Eqs. (33) and (34) can have at most one real root for θ_1 with

$$0 < \theta_1 \le \beta, \qquad \text{while} \qquad 0 < y_1 \le h. \tag{35}$$

On the other hand both the spherical nose and the optimum contour (31) are convex. There can be more than one optimum solutions with different inclinations, θ_0's. It is easier to see this by assigning $\bar{R}_0, \bar{R}_1, \beta$ and θ_1 and then solving for θ_0 from (33) and using (34) to define $\bar{l}$.

From the equations in (43), we see that the scaled wave drag of the fillet, $\bar{D}_f$, and the first term in the drag of the contour, $\bar{D}_0$ are at most $O(\beta^2)$. Using the optimum angle $\theta_1 = \theta_a$ from Eq. (48) for the optimum forebody of type a, we obtain from (43) the wave drag

$$\bar{D}_a = 0(\beta^2) + (\bar{R}_0^2/4)[1 + 0(\epsilon^{4/3})] - (3/4)\bar{R}_0^2\epsilon^{2/3} \sim \bar{R}_0^2/4 \sim \bar{D}_n. \tag{50}$$

This says, that so long as the nose radius is not too small, say $O(\sqrt{\beta})$, the leading contribution to the wave drag comes from the nose which is almost a hemisphere because $\theta_a \sim \epsilon^{2/3} << 1$.

For the optimum shape of type b we use Eq. (49) to define $\theta_1 = \theta_b$ and obtain from (43) the wave drag

$$\bar{D}_b = \bar{D}_f + (3/4)\bar{y}_1^2 \sin^2\theta_1 + 0(\beta^6) = 0(\beta^2). \tag{51}$$

This says that the contribution of the nose to the wave drag is of higher order $0(\beta^6)$ relative to the total wave drag because the azimuthal angle of the spherical nose is $\pi/2 - \theta_b \sim \epsilon$.

We used (43) and (44) to get (45), i.e., $\bar{D}_a > \bar{D}_b$. This inequality follows also from the explicit formulas (50) and (51). We note that we need the condition of $\bar{R}_0$ being not too small, (46), or rather $\bar{R}_0 >> \beta$, to establish (43) and (45). However, (43) - (45) hold for larger $\bar{R}_0$. When, $\bar{R}_0 = 0(1)$, the wave drag $\bar{D}_b$ relative to $\bar{D}_a$ is $0(\beta^2)$.

We conclude that

V, There are two optimum forebodies having the same $l, h, R_1,$ and R_0*: type a, having an almost hemispherical nose,* $\theta_a << 1$ *and type b, having a spherical nose with a small azimuthal angle,* $\pi/2 - \theta_b << 1$. *The wave drag of type b is the true minimum.*

VI, The wave drag of an optimum forebody of type b can be smaller the that of a conical body even when the nose radius $\bar{R}_0 = 0(1)$. *The wave drag of type a will be greater than that of the conical body so long as the nose radius is not too small, i.e,* $\bar{R}_0 >> \beta$.

Since the two forebodies, a and b, have the same nose radius R_0, they have the same characteristics of aerodynamic heating near the stagnation point if the effect of entropy or vorticity gradient is negligible. For the forebody of type b, the vorticity gradient will be larger than that of forebody a and thus induce at larger heat flux [2,3]. The forebody b has a relatively smaller radius of curvature $r_b < R_0$ at the junction with its nose which could effect the boundary layer. Also the nose area could be too small such that the total aerodynamic heating of the boundary layer near the stagnation point will not be sufficient to control the boundary layer downstream effectively.

A realistic comparison of the optimum forebodies a and b should include both the wave drag and viscous drag. Additional theoretical and experimental investigations on the viscous drag, in particular on boundary layer control, are needed.

Now we shall find the lower and upper bounds for the scaled length $\bar{l}$ of the forebody for a given set of $\bar{R}_0, \bar{R}_1$, andβ. For the lower bound of $\bar{l}_m(\bar{R}_0, \bar{R}_1, \beta)$, we note that the maximum value of the constant C for the optimum contour is

$$C_m = min\{sin^4\beta;\ \ 3\sqrt{3}\bar{R}_0/16\}. \tag{52}$$

When $C_m = sin^4\beta$ we have $\theta_1 = \beta$, and $y_1 = h$ for both types a and b and for all $\bar{R}_1 \geq 0$. From C_m we compute the two roots θ_a θ_b of Eq. (33) and the corresponding minimum length $(\bar{l}_m)_a$ and $(\bar{l}_m)_b$ from Eq. (34).

When $C_m = 3\sqrt{3}\bar{R}_0/16$ we have $\theta_a = \theta_b = \pi/3$ and θ_1 defined by Eq. (33). Forebody a and b coincide with each other with $\bar{l}_m$ given by Eq. (34).

There is no upper bound on the length of an forebody of type a or b, if $h + R_1 \cos\beta > R_0 + R_1$.

In case that the above condition is not valid, there exists a least upper bound on the scaled length of an optimum forebody of type a. For this type, the circular fillet and the circular nose touch the optimum contour (31) on the opposite sides of the contour in a meridian plane. The scaled length reaches its maximum, $(\bar{l}_u)_a$, when the circular nose is tangent to the circle of the fillet with $y_0 = y_1$ and the length of the optimum contour (31) vanishes. The condition on $\bar{R}_0, \bar{R}_1$ and β is

$$|C_0C_1|/h = \bar{R}_0 + \bar{R}_1. \tag{53}$$

with $|C_0C_1|$ defined by (27). The maximum $(\bar{l}_M)_a$ is the same function of $\bar{R}_0, \bar{R}_1$ and β, given by (29) for the two dimensional problem.

For the optimum forebody b, the circular fillet and the nose touch the optimum contour on the same side. There will be a least upper bound of $(\bar{l}_b$ when the circle of fillet intersects the x-axis. It occurs if $h + R_1\cos\beta - R_1 \leq 0$ and the x-intercept is $-R_1(\sin\beta + \sin\theta_1)$ where $\theta_1 = \cos^{-1}[(l + R_1\cos\beta)]/R_1]$. The least upper bound is

$$(\bar{l}_u)_b = R_1(\sin\beta - \sin\theta_1). \tag{54}$$

This upper bound is not attainable by an optimum forebody b, since the optimum solution with $\bar{l} = \bar{l}_b$ has a conical nose of cone angle θ_1 with $\bar{R}_0 = 0$.

Using the geometry of the optimum contour (31) and that of the circular nose and fillet, we can show that the scaled wave drag of a forebody a or b, with given β and $\bar{R}_0$ increases as $\bar{R}_1$ increase and/or $\bar{l}$ decreases. In the limit of $\bar{R}_1 \to \infty$, $\bar{l}$ approaches $\bar{l}^*$ of the reference forebody. Thus we can conclude

VII, The wave drag of an optimum forebody with a concave fillet, $R_1 > 0$, for either type a or b, is less than the wave drag D^* of the corresponding reference

forebody composed of a conical surface and spherical nose, with the same β, R_0 and h, while the length of the former is greater than the length l^* of the latter.

5. CONCLUDING REMARKS

Analytical solution for optimum shape of a two dimensional or axi-symmetric forebody attached to a symmetric wedge or cone of half angle β is presented. The forebody is required to have a circular nose of finite radius R_0 defined by the allowable aerodynamic heating at the stagnation point. The forebody is joined to the truncated wedge or cone at a semi-thickness or base radius h through a circular fillet to avoid a discontinuity in slope. The radius of the fillet R_1 is specified with due consideration to avoid flow separation or shock boundary layer interaction.. Using the modified Newtonian theory, optimum forebodies are defined for given set of R_0, R_1, h, β and the length of the forebody l.

Using a reference forebody, composed of the extension of the truncated wedge or cone to match with a circular or spherical nose of the same radius R_0, we show that the wave drag of an optimum forebody with a concave fillet, $R_1 > 0$, (a convex fillet $R_1 < 0$) is less (greater) than the wave drag D^* of the reference forebody while the length of the former is greater (less) that the length l^* of the latter, see statement *I*.

The optimum two dimensional and axi-symmetric forebodies with concave fillet junctions are analyzed in detail in **Secs. 3** and **4** respectively. The least upper and greatest lower bounds of the scaled length $\bar{l}$ of the forebody as functions of the parameters $\bar{R}_0, \bar{R}_1, \beta$ with h as the length scale are determined. The results are discussed under the realistic condition of $\beta \ll 1$.

For the two dimensional cases, there is an unique optimum solution for a length $\bar{l}$ within the lower and upper bounds. The optimum forebody is defined by Eqs. (25) and (27) and its wave drag by Eq. (30). The wave drag is dominated by the part on the nose which is almost a semi-circle of radius R_0 so long as $\bar{R}_0$ is not extremely small, i.e., $\bar{R} >> \beta^2$ and the reduction in drag relative to the drag of the reference forebody is small, $O(\beta^2)$ See statements *II - IV*.

For the axi-symmetric cases, there are two optimum solutions of type *a* and type *b* for an scaled length $\bar{l}$ within the upper and lower bounds. The optimum forebody is defined by Eqs. (31-34) and (40). The root of the last equation is given by (48) for type *a* and by (49) for type *b*. The wave drag is given by Eq. (43). The optimum forebody of type *a* is similar to the two dimensional case, in the sense that its nose is almost a hemisphere and its wave drag is dominated by that of the nose so long as $\bar{R}_0 >> \beta$, The optimum forebody of type *b* has a small nose in the form of a spherical cap of small azimuthal angle while the radius $\bar{R}_0$

can be 0(1). The scaled wave drag of the forebody of type b is $O(\beta^2)$ and is dominated by that of the optimum contour and the fillet while that of the nose is of much higher order. The wave drag of type b can be smaller than the drag of the conical forebody of cone angle β even when $R_0 = 0(1)$. See statements *V - VII.*

We note that our optimum solutions are based on the modified Newtonian theory. Since the surface pressure given by the modified Newtonian theory is in good agreement with the experimental data and numerical solutions of the full system of governing equations, we can introduce a small positive parameter

$$\delta << 1$$

to denote the order of magnitude of the error of the surface pressure coefficient predicted by the modified Newtonian theory. Then *the wave drag given by the experiment or by the numerical solution using our optimum forebody will differ from the true minimum by* $0(\delta^2)$. In other words, the "true" optimum shape will be small perturbation from our optimum shape. Instead of search for the "true" optimum shape directly by numerical solution it is much easier to determine the small perturbation numerically.

It should also be noted that in addition to the wave drag we should also include the viscous drag. The latter requires a careful study of the boundary layer, flow transition and/or separation. Our optimum forebodies are simple and could serve as basic models for systematic experimental studies of the effects of the scaled length and nose radius on the total drag and their effects on the strong interaction of boundary layer with entropy layer and on the boundary layer control by utilizing aerodynamic heating near the stagnation point.

References

[1] Hayes, W. D. and Probstein, R. F., "Hypersonic Flow Theory," Vol. J. "Inviscid Flows," Academic Press, 1966, pp. 152-168, 401-402.

[2] Fay, J. A. and Ridell, F. R., "Theory of Stagnation Point Heat Transfer in Dissociated Air," Journal Aero. Sc., Vol. 25, No. 2, February 1958, pp. 73-85.

[3] Ferri, A., Zakkay, V., and Ting, L., "Blunt-Body Heat Transfer At Hypersonic Speed and Low Reynolds Number," Journal Aero. Sc., Vol. 28, No. 12, December 1961, pp. 962-872.

[4] Ferri, A., Zakkay, V. and Ting, L., "On Blunt-Body Heat Transfer at Hypersonic Speed and Low Reynolds Numbers," Journ. Aero. Sc., Vol. 29, No. 7, July 1962, pp. 882-883.

[5] Liepmann, H. W. and Nosenchuck, D. M., "Active Control of Laminar-Turbulent Transition," J. Fluid Mech., Vol. 118, May 1982, pp. 1878-200.

[6] Maestrello, L. and Ting, L., "Analysis of Active Control by Surface Heating," AIAA J., Vol. 23, No. 7, July 1985, pp. 1038-1045.

[7] Maestrello, L., "Active Transition Fixing and Control of the Boundary Layer in Air," AIAA J., Vol. 24, No. 10, October 1986, pp. 1577-1581.

[8] Maestrello, L., Badavi, F. F., and Noonan, K. W., "An Application of Active Surface Heating for Augmenting Lift and Reducing Drag of An Airfoil," NASA TM 100563, March 1988.

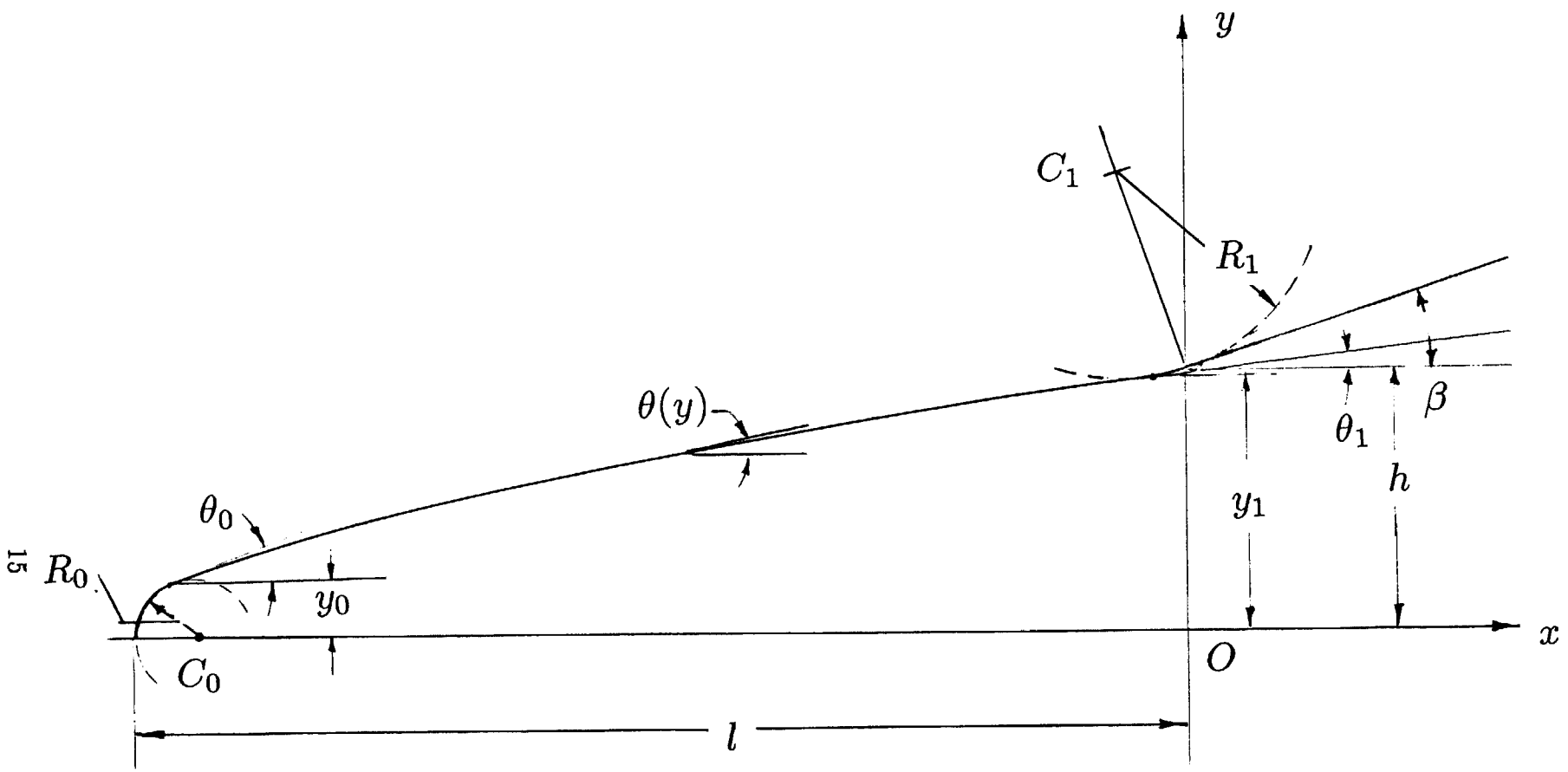

Figure 1. Geometry of an Optimum Forebody attached to a wedge or cone.

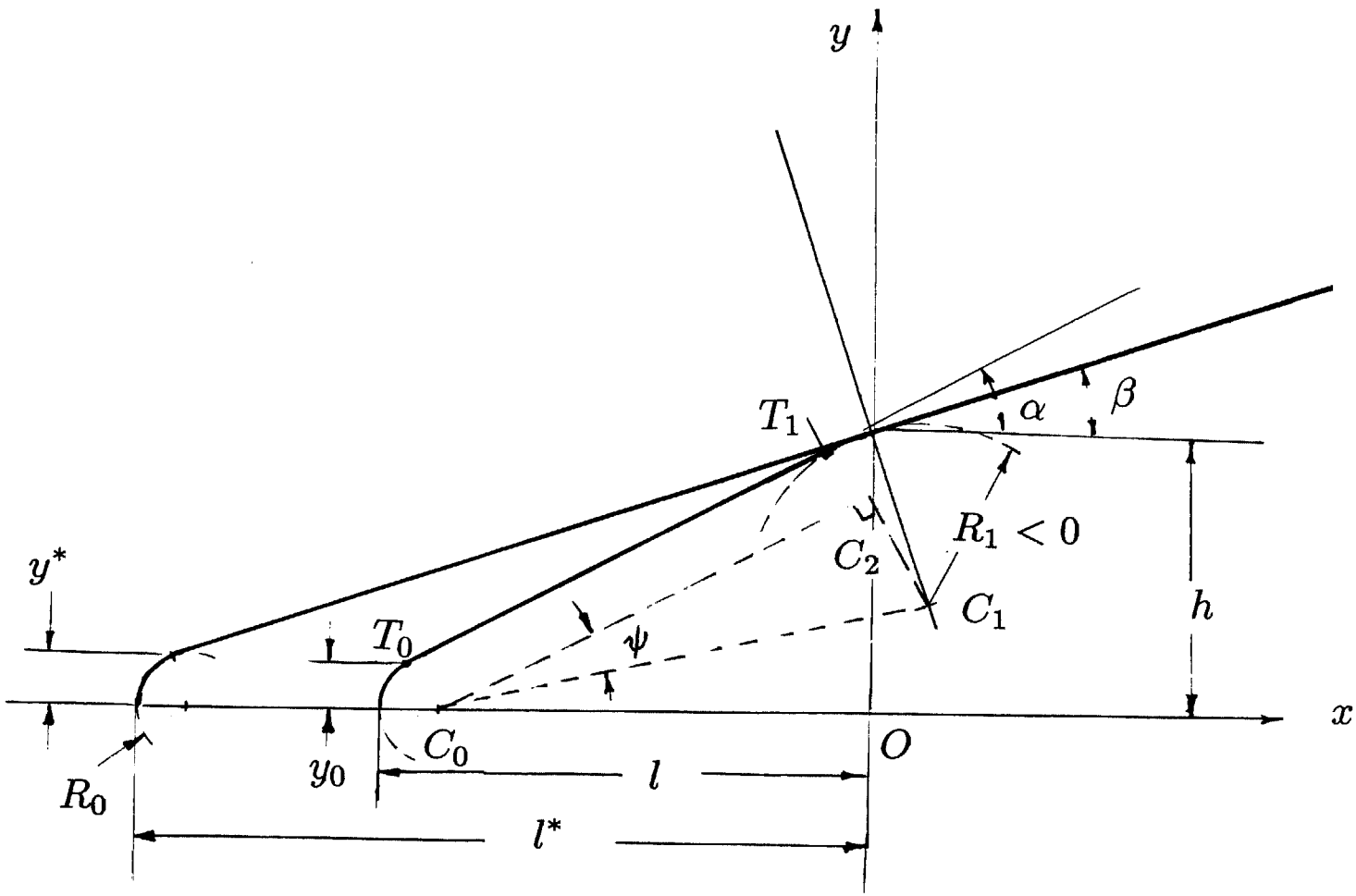

Figure 2. Optimum forebodies with a convex fillet joint to the wedge of cone and the reference forebody.

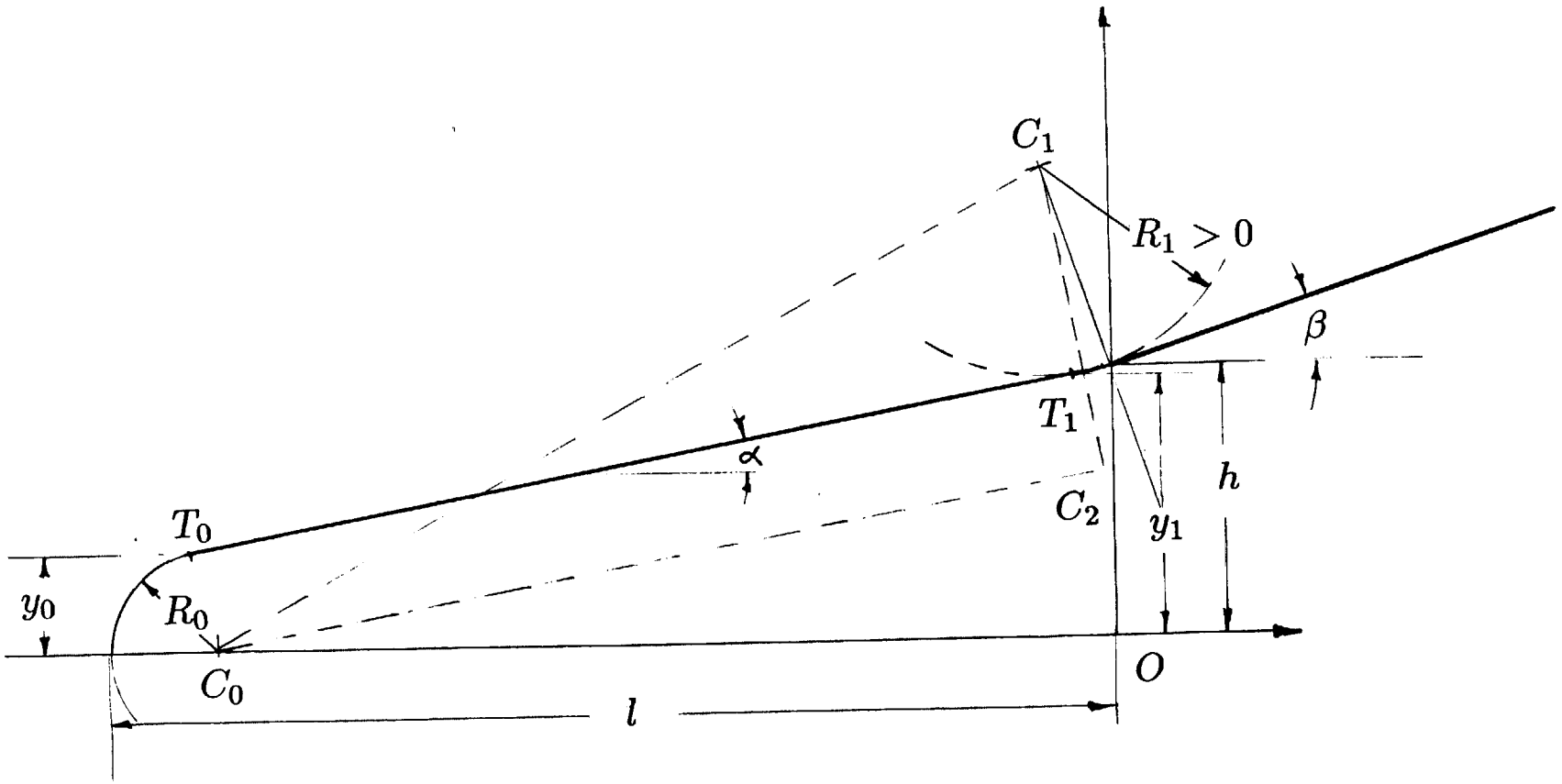

Figure 3. Optimum two dimensional forebodies with concave fillets.

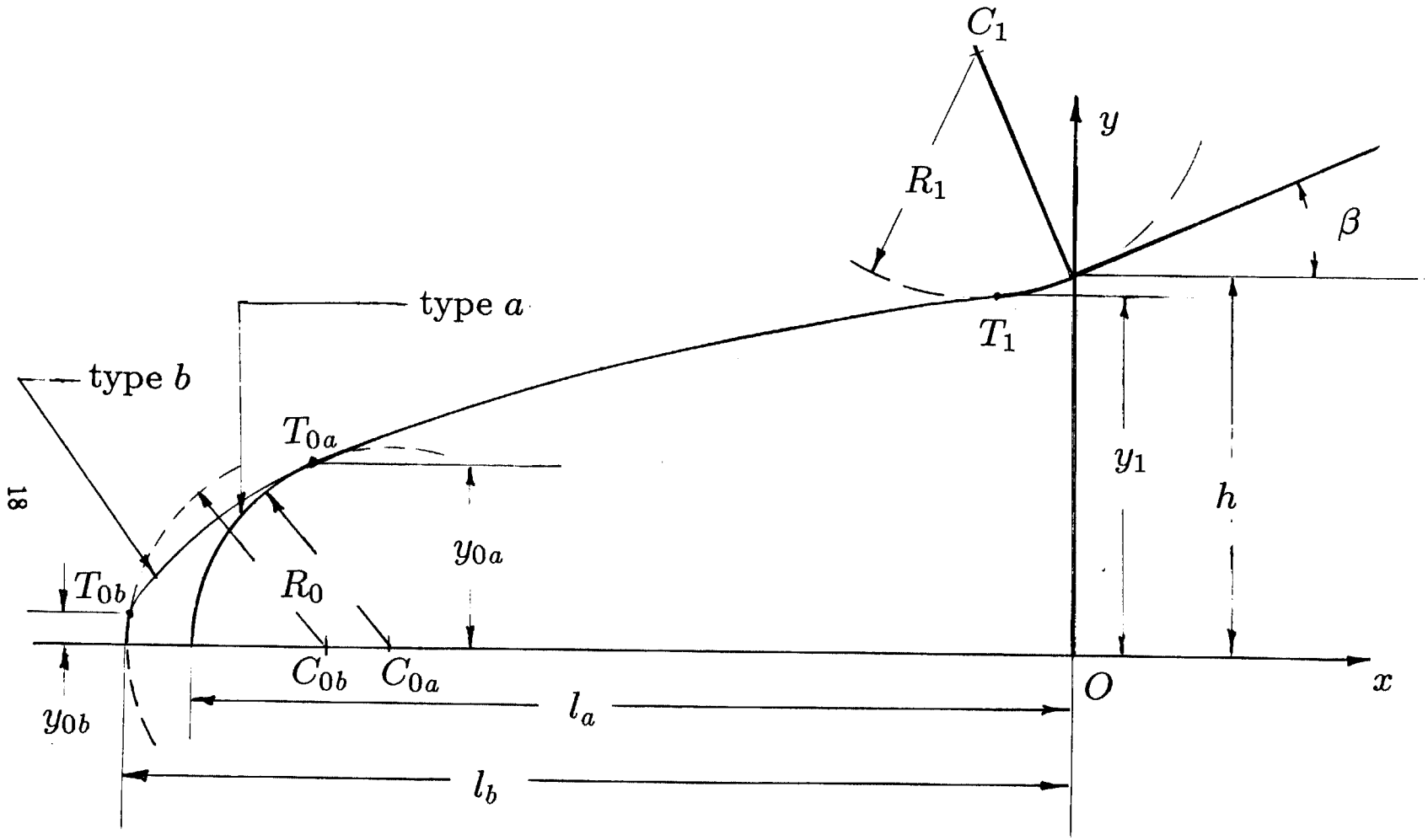

Figure 4. Optimum Axi-symmetric forebodies with the same concave fillet length.

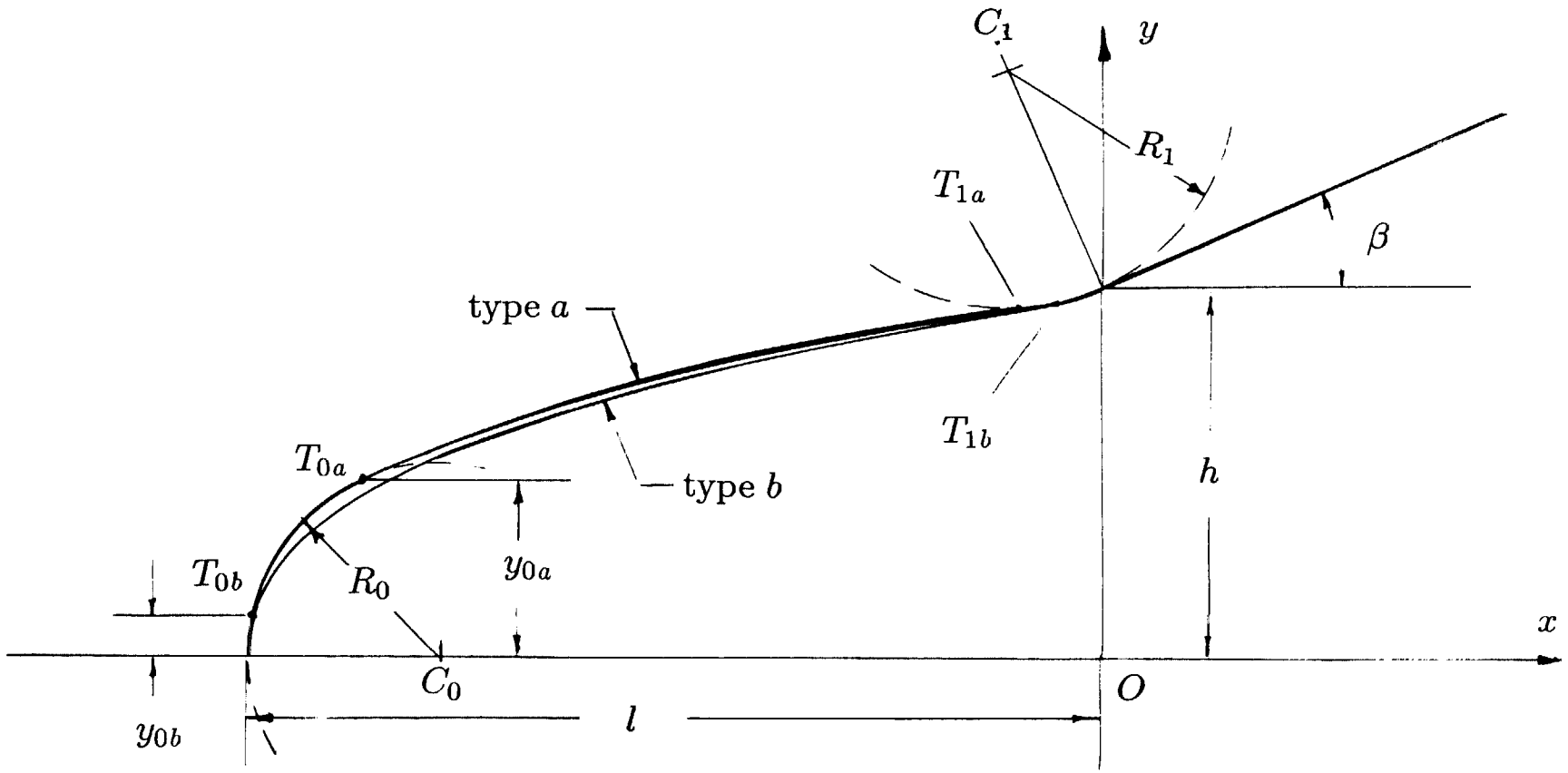

Figure 5. Optimum Axi-symmetric forebodies with the same length.

NASA
National Aeronautics and Space Administration

Report Documentation Page

1. Report No.	2. Government Accession No.	3. Recipient's Catalog No.
NASA CR-181955 ICASE Report No. 89-51		

4. Title and Subtitle	5. Report Date
OPTIMUM SHAPE OF A BLUNT FOREBODY IN HYPERSONIC FLOW	December 1989
	6. Performing Organization Code

7. Author(s)	8. Performing Organization Report No.
L. Maestrello L. Ting	89-51
	10. Work Unit No. 505-90-21-01

9. Performing Organization Name and Address	11. Contract or Grant No.
Institute for Computer Applications in Science and Engineering Mail Stop 132C, NASA Langley Research Center Hampton, VA 23665-5225	NAS1-18605
	13. Type of Report and Period Covered: Contractor Report

12. Sponsoring Agency Name and Address	14. Sponsoring Agency Code
National Aeronautics and Space Administration Langley Research Center Hampton, VA 23665-5225	

15. Supplementary Notes

Langley Technical Monitor:
Richard W. Barnwell

Final Report

16. Abstract

The optimum shape of a blunt forebody attached to a symmetric wedge or cone is determined. The length of the forebody, its semi-thickness or base radius, the nose radius and the radius of the fillet joining the forebody to the wedge or cone are specified. The optimum shape is composed of simple curves. Thus experimental models can be built readily to investigate the utilization of aerodynamic heating for boundary layer control. The optimum shape based on the modified Newtonian theory can also serve as the preliminary shape for the numerical solution of the optimum shape using the governing equations for a compressible inviscid or viscous flow.

17. Key Words (Suggested by Author(s))	18. Distribution Statement
Hypersonic flow, optimum shape	02 - Aerodynamics Unclassified - Unlimited

19. Security Classif. (of this report)	20. Security Classif. (of this page)	21. No. of pages	22. Price
Unclassified	Unclassified	21	A03